When Energetic Materials, PDMS-Based Elastomers, and Microelectronic Processes Work Together: Fabrication of a Disposable Microactuator

Samuel Suhard,[†,‡] Pierre Fau,[†] Bruno Chaudret,[†] Sylviane Sabo-Etienne,*[,†] Monique Mauzac,[‡] Anne-Françoise Mingotaud,*[,‡] Gustavo Ardila-Rodriguez,[§] Carole Rossi,[§] and Marie-Françoise Guimon[||]

CNRS, Laboratoire de Chimie de Coordination, Université de Toulouse, UPS, INPT, 205 route de Narbonne, F-31077 Toulouse, France, Laboratoire des IMRCP, CNRS, UMR 5623, Université de Toulouse, 118 route de Narbonne, 31062 Toulouse Cedex, France, LAAS-CNRS, Université de Toulouse, 7 Avenue Du Colonel Roche, 31077 Toulouse Cedex 4, France, and IPREM-ECP, UMR 5254, Hélioparc Pau-Pyrénées, 2 Avenue Pierre Angot, 64053 Pau Cedex 9, France

Received November 19, 2008. Revised Manuscript Received February 3, 2009

The present article describes the elaboration of a microactuator based on the decomposition of an energetic material. The fabrication of such a pyrotechnic actuator relies on novel smart materials and a simplified process developed through chemistry. The heterometallic Werner complex $[Co(NH_3)_6]_2[Mn(NO_3)_4]_3$ was chosen as an energetic material releasing only biocompatible gases when ignited. It was deposited on a resistance at the bottom of a micrometer scale chamber comprising directly photocurable polydimethylsiloxane walls and a thin elastic membrane as a roof. The membrane also comprised polysiloxanes. One of the key steps consisted of the grafting of siloxane-bearing acrylate moieties onto a standard silicon wafer, similar to those incorporated on the polysiloxane. The grafting was successfully characterized by XPS. Moreover, the walls of the cavity were elaborated by direct photolithography. After deposition of the energetic material, the cavity was sealed thanks to membrane grafting and the process was optimized to afford strong wafer/wall and wall/membrane interfaces in order to withstand the high mechanical stress imposed on the device in use.

Introduction

During the past decades, the development of microactuators has led to a wide variety of devices with applications in the fields of chemical analysis, biological sensing, and drug delivery in chemical, biological, and medical industries. The systems are becoming increasingly sophisticated and rely to a larger extent on new and smart materials developed through chemistry. Keller et al. have reported on the fabrication of artificial muscles based on such new and smart materials: a nematic liquid crystal elastomer.[1] Their work is particularly interesting, because the use of a liquid crystal elastomer fits perfectly with the standard soft lithography process for the fabrication of a microactuator. Tetra[2,3-thienylene] constitutes another smart material that was efficiently utilized as a single molecule electromechanical actuator.[2]

There is a particular interest in actuators with a potential use as disposable microsyringes. Within this field, there exist numerous systems in which various sources of actuation have been employed: electrostatic, piezoelectric or thermopneumatic actuation.[3] The complexity of such systems is one of their main disadvantages, in addition to their high cost and their nondisposable use. For one-shot syringe applications, pyrotechnic actuators appear to be an interesting alternative.[4] They often rely on the decomposition of a chemical compound which generates gas. Beaucage et al. have, for instance, reported on the fabrication of such devices that involved 2,2′-azobisisobutyronitrile (AIBN) as the propellant.[5] The fabrication of the microactuator was straightforward, constituting a three-step process: constructing the heater, depositing the solid propellant, and encapsulating the resulting device. In this system, when AIBN is heated at 70 °C, nitrogen is released and becomes the source of actuation. Although this method provides a portable and disposable actuator in few steps, AIBN may not be the best propellant for mass production because of its relative instability and low activation temperatures. Choi et al. proposed another pyrotechnic micropump actuated through the catalyzed decomposition of hydrogen peroxide by manganese oxide in oxygen and water.[6] Again, the technical process was relatively simple (4 steps), but the deposition of MnO_2 is tricky and requires layers of parafilm to separate

* Corresponding author. E-mail: sylviane.sabo@lcc-toulouse.fr (S.S.-E.); afmingo@chimie.ups-tlse.fr (A.-F.M.).
[†] Laboratoire de Chimie de Coordination, Université de Toulouse.
[‡] Laboratoire des IMRCP, Université de Toulouse.
[§] LAAS-CNRS, Université de Toulouse.
[||] Hélioparc Pau-Pyrénées.

(1) Buguin, A.; Li, M. H.; Sillberzan, P.; Ladoux, B.; Keller, P. *J. Am. Chem. Soc.* **2006**, *125*, 1088–1089.
(2) Marsella, M. J.; Reid, R. J.; Estassi, S.; Wang, L. S. *J. Am. Chem. Soc.* **2002**, *124*, 12507–12510.
(3) Nisar, A.; Afzulpurkar, Mahaisvariya, N. B.; Tuantranont, A. *Sens. Actuators, B* **2008**, *130*, 917–942.
(4) Rossi, C.; Estève, D. *Sens. Actuators, B* **2005**, *120*, 297–310.
(5) Hong, C. C.; Murugesan, S.; Kim, S.; Beaucage, G.; Choi, J. W.; Ahn, C. H. *Lab Chip* **2003**, *3*, 281–286.
(6) Choi, Y. H.; Son, S. U.; Lee, S. S. *Sens. Actuators, A* **2004**, *111*, 8–13.

10.1021/cm803146y CCC: $40.75 © 2009 American Chemical Society
Published on Web 02/18/2009

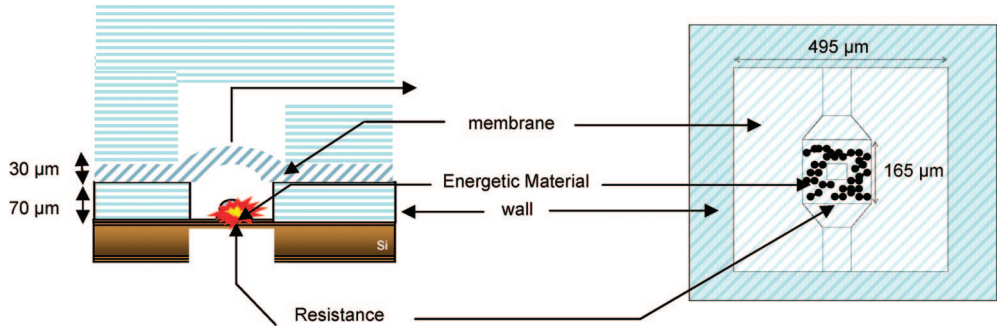

Figure 1. Schematic representation of the actuator. Left: Transversal view of the microactuator. Right: Top view of the actuator.

the catalyst from H_2O_2. Failure to obtain this separation would lead to an immediate initiation of the H_2O_2 decomposition. The generated gases are interesting as they are biocompatible; however, hydrogen peroxide is known to have a limited stability in time and is not very suitable for mass production of disposable syringes.

To the best of our knowledge, all the actuators listed above as well as those relying on PDMS-based materials, mainly imply the use of molds that first need to be obtained by regular photolithography using photoresists such as SU-8 or Shipley SJR5740.[7−9] Although this method is reliable, we preferred the development of a negative PDMS photoresist to minimize transfer and alignment steps, thereby simplifying the technical process. As a result, a PDMS actuator could be directly prepared by photolithography. Furthermore, SU-8 could not be used directly as the material for the walls because of compatibility problems of chemical functionalities with PDMS membrane.

The strategy behind the present investigation was thus to design a reliable microactuator based on "clean energetic materials" and directly photocurable PDMS. The microactuator was based on four parts as depicted in Figure 1: the heating resistance, the energetic material, the walls, and the membrane. According to the strategy, a large quantity of gas was to be generated following the decomposition of the energetic material, thereby giving rise to a deformation of the elastic membrane, and finally leading to the liquid being pushed inside the tubing.

The technical details of the actuator have been published elsewhere.[10] From a chemical point of view, several problems had to be addressed. First, a suitable energetic material needed to be selected and synthesized in easily accessible conditions.[11] The material then had to be deposited onto the device. The material's temperature sensitivity was an important parameter when designing the actuator. Second, the choice of material constituting the walls and membranes was very important. To shorten the process, it was decided that the walls should be obtained directly by photolithography without the use of molds. Because of the mechanical stress imposed onto the device when utilized, a very strong attention was paid to the wafer/wall and wall/membrane interfaces. Naturally, the membrane also had to be elastomeric and compatible with the walls. We present here the three main steps leading to the device presented in Figure 1: the deposition of the energetic material onto the resistance, the synthesis of the walls, and the fabrication of the membrane, with a specific emphasis on the problem of interface adhesion.

Experimental Section

General Information. Operations were conducted under air unless stated otherwise. Solvents were freshly distilled under nitrogen from sodium (toluene), or from calcium hydride (dichloromethane). Silver nitrate and hexaamminecobalt trichloride were purchased from Alfa Aesar, stored and used without further purification. $MnCl_2$ was obtained from Merck and dried over P_2O_5 under vacuum at 120 °C for two days, after which it was stored in a dry box. RMS 083 and acryloxypropyltrimethoxysilane were purchased from ABCR, stored at 4 °C and used without further purification. Sylgard 184 was available from Dow Corning. The photoinitiator Irgacure 2100 was generously donated by Ciba. Oxygen plasma was performed in a Pico UHP Diener plasma chamber. SiO_2-coated wafers (Si:525 μm + 1.4 μm SiO_2) were provided by the LAAS laboratory. UV irradiation was performed on a 100 W black ray lamp or with an EVG 620 mask aligner. The irradiation was carried out at 365 nm and the power of the lamps was 20 mW/cm^2. Contact angle measurements were conducted on a GBX Digidrop Fast/60 machine operating on Windrop. Thicknesses were determined with a profilometer (KLA Tencor P.15) and scanning electron microscopy was performed on a Hitachi S4800 instrument. Thermal data were collected on a Setaram TGA-DTA 92 microbalance equipped with a temperature control device CS 92 under a helium atmosphere. Samples were prepared in closed alumina crucibles. Microanalyses were performed by the LCC microanalytical service.

Heating Platform. The heating resistance was based on a silicon platform process developed by the LAAS laboratory[12] consisting of low-pressure chemical vapor deposition (LPCVD), plasma enhanced chemical vapor deposition (PECVD), arsenic and phosphorus implementation atoms, as well as etching techniques (see the Supporting Information for further details).

X-ray Photoelectron Spectroscopy (XPS). XPS spectra were conducted in IPREM-ECP using an SSI M-Probe (model 301) spectrometer at room temperature. A monochromatic Al Kα X-ray

(7) Xia, Y.; Whitesides, G. M. *Angew. Chem., Int. Ed.* **1998**, *37*, 550–575.
(8) Fu, A. Y.; Chou, H. P.; Spence, C.; Arnold, F. H.; Quake, S. R. *Anal. Chem.* **2002**, *74*, 2451–2457.
(9) Unger, M. A.; Chou, H. P.; Thorsen, T.; Scherer, A.; Quake, S. R. *Science* **2000**, *288*, 113–116.
(10) Ardila-Rodriguez, G. A.; Suhard, S.; Rossi, C.; Estève, D.; Fau, P.; Sabo-Etienne, S.; Mingotaud, A. F.; Mauzac, M.; Chaudret, B. *J. Micromech. Microeng.* **2008**, *19*, 015006.
(11) Pradère, C.; Suhard, S.; Vendier, L.; Jacob, G.; Chaudret, B.; Sabo-Etienne, S. *Dalton Trans.* **2008**, *20*, 2725–2731.
(12) Rossi, C.; Boyer, P. T.; Estève, D. *Sens. Actuators, A* **1998**, *64*, 241–245.

(1486.6 eV) was employed for the excitation. High-resolution spectra were recorded at constant pass energy of 50 eV. The analysis chamber pressure was on the order of $\sim 1 \times 10^{-7}$ Pa. Experimental and theoretical bands were fitted (80% Gaussian and 20% Lorentzian) using a nonlinear baseline with a least-squares algorithm. Moreover, binding energies were determined with an experimental error of ± 0.2 eV.

Synthesis of $[Co(NH_3)_6]_2[Mn(NO_3)_4]_3$.[11] Under air, $MnCl_2$ (0.30 g, 2.38 mmol) was dissolved in water (5 mL), after which $AgNO_3$ (1.62 g, 9.56 mmol) was added and AgCl precipitated. The reaction was stirred for 5 min, and a further 10 mL of water were added. Subsequently, $[Co(NH_3)_6]Cl_3$ (0.42 g, 1.59 mmol) was charged to the mixture with the concomitant precipitation of AgCl. The solution turned orange, and the reaction was stirred for 5 min, filtered through celite, and washed with water (10 mL). The filtrate was recovered and the water removed under a vacuum to yield a solid that was subsequently dried over P_2O_5 and under a vacuum for 18 h. The result was an orange solid, 560.2 mg, 57%. (Found: C, 0.3; H, 2.9; N, 26.0%. Anal. Calcd for $Co_2Mn_3N_{24}H_{36}O_{36}.3(H_2O)$ requires: C, 0; H, 2.9; N, 26.2%.)

Functionalization of the Wafers. SiO_2-coated Si wafers (2 cm $\times$ 2 cm or 4-in full wafer disks) were washed with acetone (5 mL), dried under a N_2 flux, sonicated in isopropanol for 10 min, dried again, and sonicated for another 10 min in dichloromethane, after which they were finally dried under an N_2 flux. The wafer was placed in an oxygen plasma (140 W) oven for 30 min and was immediately immersed in water, dried under a vacuum, and placed under argon. The wafer (2 cm $\times$ 2 cm) was placed in a glass reactor under argon and 5 mL of toluene were added followed by 0.25 mL of acryloxypropyltrimethoxysilane. The resulting mixture was heated at 120 °C for 18 h. The toluene solution was removed with a double-tipped needle, and 5 mL of CH_2Cl_2 were added. The reactor was then sonicated for 5 min. The solvent was again removed and the washing procedure was repeated twice. Finally, the wafer was dried under vacuum. For the 4 in. wafers, quantities were multiplied by 10.

Deposition of the Polymer, Photocrosslinking, and Deposition of the Membrane. RMS 083 and Irgacure 2100 (2% w/w) were deposited on a wafer using a spin-coater (1000 rpm, 1000 rpm/s, 30s), and this was followed by UV curing for 30 min (lamp-wafer distance: 9 cm). To assess the adhesion between the polymer and the wafer, we immersed the system in a hexane bath and sonicated it for 15 min. For cases of poor adhesion, the polymer film was observed to separate from the support. Furthermore, for the microstructures built on the 4 in. silicon wafers, the operation was carried out with an EVG 620 mask aligner. The UV cure time was, in this case, 15 min (mask-wafer distance: 100 μm). For the elaboration of the membrane, Sylgard 184 (10/1) or Zipcone TR was deposited on a wafer with a polyethyleneterephthalate (PET) layer using a spin-coater (1000 rpm, 1000 rpm/s, 30s). This was followed by a partial cross-linking at 65 °C for 4 min before transferring it to the other part of the device.

Actuation. Characterization of the actuation was carried out by applying a tension with a KEITHLEY 2612 sourcemeter on the resistance. The resulting deformation of the membrane was analyzed by optical profilometry (FOGALE ZOOMSURF 3D).

Results and Discussion

Energetic Material. Previous research efforts comprise the development of new energetic materials for airbags.[11] These compounds are heterometallic Werner complexes and were found to be the most suitable compounds for the microactuator as a result of their properties, particularly their temperature decomposition control leading to the release of nontoxic metallic oxides and environmentally friendly gases: H_2O, N_2, O_2.

Scheme 1. Synthesis of the Energetic Materials

$$3MnCl_2 + 2Co(NH_3)_6Cl_3 + 12AgNO_3 \xrightarrow[H_2O]{} [Co(NH_3)_6]_2[Mn(NO_3)_4]_3 + 12AgCl$$

Two paths are available for the synthesis of such heterometallic complexes: a multistep organic approach or a one-step aqueous route in air. The aqueous route is very interesting because of its simplicity and the fact that it can be easily reproduced in a clean room environment by a nonspecialist. A cobalt−manganese compound, prepared according to Scheme 1, was thus selected.

A very important characteristic of the energetic material is the oxygen balance (%), corresponding to the number of moles of oxygen released per mole of initial energetic material. This oxygen balance must be positive (11.7%) in order for a full combustion to occur, which in turn is crucial for possible applications in biology. The heterometallic energetic compounds could be easily characterized by thermogravimetric analysis, resulting in the observation of a straight and clean decomposition. The initiation temperature was found to be 223 °C (see Figure 2) and the decomposition reaction is presented in Scheme 2. As a result of the choice of ligands, only nontoxic gases were formed. It was indeed important to avoid the use of carbon ligands in order to prevent the formation of CO or CO_2. The initiation temperature demonstrated a perfect fit with regard to the criteria required for the application: it was high enough for actuation to take place and easily attainable by the microresistance. A movie corresponding to the decomposition of the energetic material can be found in the Supporting Information.

The amount of energetic material required for a high deformation of the top elastomeric membrane was found to be ca. 850 ng according to a modeling study of the microactuator.[13] The preparation of a water solution proved to be a very convenient and safe means of depositing such small amounts. The energetic materials that were used are highly soluble in water and were therefore deposited in solution (127 mg, 1.3 mL) by drop deposition through a glass capillary. Crystalline energetic materials could thus be readily obtained on the resistance by rapid water evaporation at room temperature. This technique proved to be reliable when

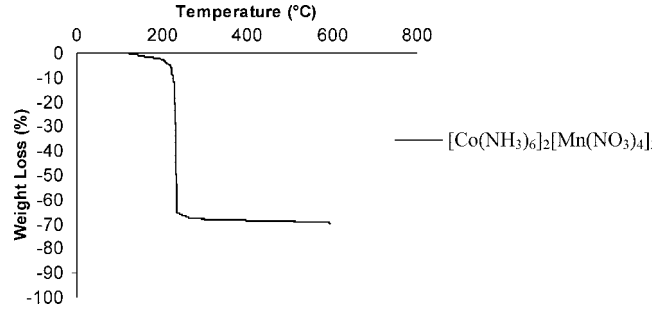

Figure 2. Thermogravimetric analysis of the $[Co(NH_3)_6]_2[Mn(NO_3)_4]_3$ complex.

Scheme 2. Decomposition of the Energetic Material

$$[Co(NH_3)_6]_2[Mn(NO_3)_4]_3 \longrightarrow Co_2O_3 + 3\ MnO_2 + 18\ H_2O + 12\ N_2 + 9/2\ O_2$$

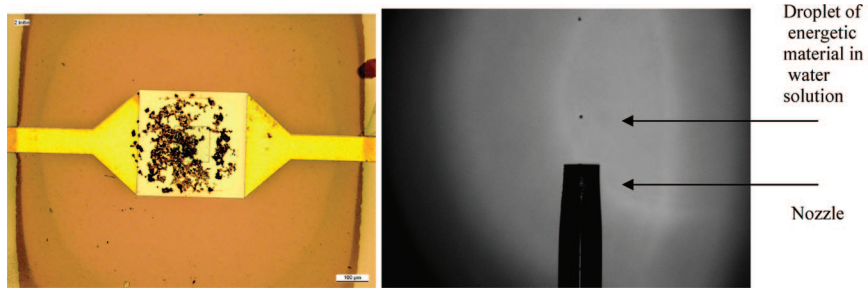

Figure 3. Deposition of the energetic material on the heating resistance. Left: when using a capillary (scale bar: 100 μm). Right: when using an inkjet apparatus.

utilizing the same glass capillaries and was therefore chosen for the fabrication of the first microactuator prototype. Subsequently, an automatic inkjet apparatus was employed, allowing the dispensation of 30 μm solution droplets. This technique gives rise to a highly localized deposition and avoids the dispersion of the energetic material upon water evaporation. In addition, inkjet deposition is extremely fast: a 4 in. wafer with 320 dies can be processed in 10 min, thus opening the way for a possible industrial scale-up. Figure 3 depicts energetic materials deposited by a capillary (left) and the stroboscopic picture of a water droplet of the energetic material being dispensed by the inkjet apparatus (right).

Walls. Because of their wide use and easy access for microtechnologies, silicone-based materials were chosen for the walls and the elastic membrane. There already exist several reports of layered devices utilized for microfluidic applications, thus proving that a very good compatibility could be achieved during the process. The aim was therefore to design a photolithographic process with polysiloxane polymers without the use of a mold and to ensure their irreversible covalent bonding onto Si wafers. Although polysiloxanes are widely employed in microtechnology, only a few examples in the literature have adressed the problem of photopatternable polysiloxanes. The first one was proposed by Lötters et al. and concerned a commercial polysiloxane bearing methacrylate groups and a primer to increase the bonding between the wafer and the polymer.[14,15] No characterization of the modified surface was presented and the photopolymerization needed to be performed in the absence of oxygen. Rogers et al. presented the synthesis of a modified polysiloxane comprising long segments of PDMS as well as short ones bearing methacrylate groups.[16] This polymer has the advantage of exhibiting a lower shrinking upon cross-linking, but is not commercially available. Very recently, Papautsky et al. proposed a clever use of the popular Sylgard 184 (see Figure 7) to render it photosensitive.[17] The proposed method was quite elegant, but included several difficult points. Indeed, in order to obtain well-defined patterns, the optimal baking time and baking temperature should be well-controlled and determined for each new system. In fact,

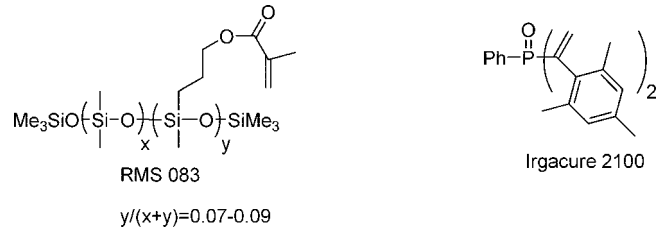

Figure 4. Chemical formula of the polymer and the corresponding photoinitiator.

overbaking causes some of the exposed areas to be cross-linked. Similarly, a slightly higher temperature would cause the same defects to the material. This problem of photopatternable polysiloxanes was also examined by Dow Corning, a company that has provided such polymers since a few years back.[18] The basic chemistry remains that of hydrosilylation reactions that become facilitated in the presence of a photoreagent under UV irradiation. However, this methodology still necessitates a soft baking prior to the UV treatment followed by a postexposure baking in order to complete the synthesis of the material. Moreover, available thicknesses lie between 6 and 50 μm. Depending on the application, this range is not large enough.

The present research effort includes the development of a strategy to obtain photopatternable PDMS walls around the heating element through the functionalization of the surface of a SiO_2-coated Si wafer with photoreactive methacrylate moieties. A copolymer of dimethyl and methacryloxypropylmethyl siloxane, RMS 083, from Gelest, was chosen for the investigation and its chemical structure is presented in Figure 4. The percentage of methacrylate monomer units is somewhere between 7 and 9% and the viscosity of this polymer lies in the range of 2000−3000 cSt, which corresponds to a molecular weight of approximately 40 000 g mol^{-1}.

The issue of obtaining surface functionalization is not new and numerous methods have been developed.[19] Glass is the most studied surface because of its very low cost and the presence of potentially reactive Si-OH surface groups. The functionalization of a silica surface involves two steps: the generation of the largest possible number of silanol groups (SiOH) and a reaction with the desired grafting agent **1** (see Scheme 3).

(13) Ardila Rodríguez, G. A. PhD Thesis, Université Paul Sabatier, Toulouse, France, 2008.
(14) Lötters, J. C.; Olthuis, W.; Veltink, P. H.; Bergveld, P. *J. Micromech. Microeng.* **1997**, *7*, 145–147.
(15) Lötters, J. C.; Olthuis, W.; Veltink, P. H.; Bergveld, P. *Microsystem Technol.* **1997**, 64–67.
(16) Choi, K. M.; Rogers, J. A. *J. Am. Chem. Soc.* **2003**, *125*, 4060–4061.
(17) Bhagat, A. A. S.; Jothimuthu, P.; Papautsky, I. *Lab Chip* **2007**, *9*, 1192–1197.
(18) http://www.dowcorning.com/content/etronics/etronicspattern/etronicspattern_photoov.asp.
(19) Arkles, B. *Silane Coupling Agents: Connecting Across Boundaries*; Gelest: Morrisville, PA, 2006; catalog and references therein.

Scheme 3. Grafting of Acryloxypropyltrimethoxysilane on Si Wafers

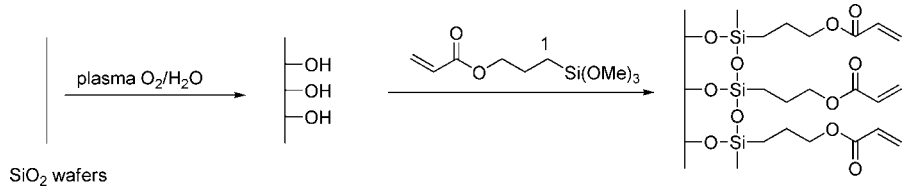

Oxygen plasma has been shown to cleave Si−O−Si bonds leading to the formation of Si−O species.[20] A treatment with water blocks these reactive functions into silanols that can be kept for short times (typically an hour or so). The silanols can then be used in a subsequent reaction with the grafting agent. The procedure has the advantage of being clean, secure, and fairly quick (30 min), and for these reasons, the hydroxylation was performed by plasma and was followed by a toluene solution of compound **1** being refluxed overnight. The surface of such modified wafers was then analyzed by contact angle experiments and the contact angles were found to be 47.0° (±1.7° in 10 measurements) and 68.9° (±1.5° in 10 measurements) before and after treatment, respectively. These results clearly demonstrate that the surface of the wafer increased in hydrophobicity after treatment, which represented a strong indication that compound **1** had become anchored. No further modifications of the contact angles were observed during the following hour, signifying a stable chemical modification.

The characterization of the surface anchoring was achieved by XPS analyses,[21−23] and the observed spectra can be seen in Figure 5. The spectrum shown in Figure 5a (left) indicates a relatively thick oxide layer. Since no band at 99 eV corresponding to Si^0 is visible, it was concluded that only SiO_2 was present after the plasma treatment. C−C and C−O bonds, on the other hand, were found to be present before the treatment because of carbon contamination (Figure 5a, right). After treatment by **1**, a new band appeared at 102 eV which was attributed to O−Si−C bonds (b, left). Moreover, in the carbon area, a new band corresponding to O−C═O bonds was observed at 288 eV (b, right). These data demonstrate the effective grafting of compound **1** onto the silicon wafers.

Photopatternization of PDMS. Having demonstrated the presence of reactive acrylate moieties on the wafer surface, the next step was to anchor the RMS 083 onto the silicon wafer. For this, a commercial material was chosen in order to have access to PDMS layers of at least of 50 μm, which was needed for the elaboration of the desired microactuator. Indeed, there exist several commercial kits of PDMS that can be UV-cross-linked. However, such polymers are often very fluid and their deposition by spin coating affords only thin films. In the present case, the goal was to synthesize a 500 μm × 500 μm square cavity in PDMS with a thickness between 50 and 200 μm, which was to surround a resistance in the final device. Consequently, a mixture of RMS 083 with the initiator Irgacure 2100 (2% w/w, a typical value for photoinitiators) was deposited by spin coating. Irgacure 2100 (cf. Figure 4) was selected because its absorbing range was compatible with the polymer as well as with the existing instruments in the laboratory. Furthermore, it had the advantage of being in liquid form, thus facilitating its incorporation into the polymer. As compared to the initiator described by Lötters, for which setting during a full night was recommended,[14,15] Irgacure 2100 can be used immediately. The parameters of the spin coater (i.e., the speed, acceleration, and time) were varied in order to obtain a range of thicknesses. The resultant wafers were exposed to UV−visible light for 30 min, after which the thickness was determined by profilometry with a typical accuracy of 1% (Table 1).

According to Table 1, the desired thickness could indeed be obtained, which demonstrated the tunability of RMS 083. This material was thus considered to be an interesting alternative to other commercially available PDMS grades. Mixtures of RMS 083 and Irgacure 2100 (2 wt %) were deposited (1000 rpm, 1000 rpm/s, 30s) on the functionalized wafers bearing acrylate groups. Structuration of this layer was then performed by classical photolithographic processes using UV−visible light at 365 nm for 15 min, through dedicated glass patterned masks followed by development in methylisobutylketone (MIBK):isopropanol (IPA), 1:1 vol/

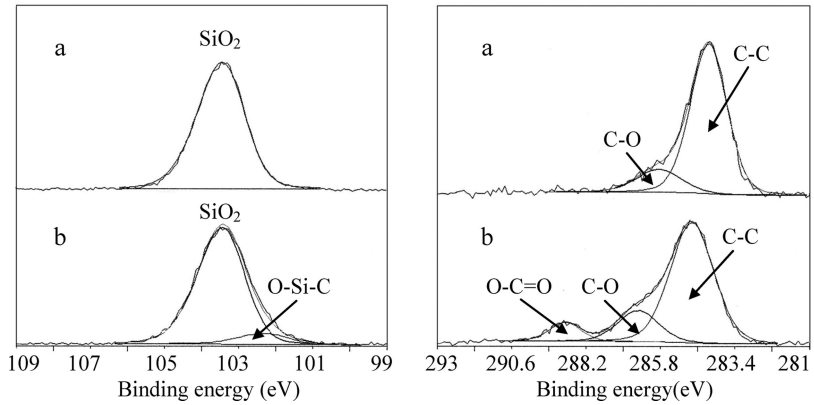

Figure 5. XP spectra (left side, Si2p; right side, C1s) of acrylate functionalized wafers. (a) Wafer treated by oxygen plasma before functionnalization. (b) Same wafer after functionnalization.

Table 1. Control of the Polymer Layer Thickness by Spin Coating

speed (rpm)	acc (rpm/s)	time (s)	thickness (μm)
250	250	30	305
400	400	30	240
1000	1000	30	120
2000	2000	30	35

vol (see the Supporting Information). After the curing, the adhesion of the polymer films was assessed by placing the wafers in 10 mL of hexane in an ultrasound bath for 10 min. In the case of a poorly grafted film, this treatment led to the peeling of the film from the surface. Such a method was chosen because it seemed more reliable than simple manual peel tests. In the case of wafers treated by **1**, no random peeling was observed on the surface of the wafer, thereby demonstrating a perfect adhesion.

It is noteworthy that no negative resin was used in this process to create a preliminary mold. After a successful optimization of the adhesion, a SiO_2-coated wafer, priorly treated with compound **1**, was subjected to the above-mentioned process and the result was that well-defined cavities could indeed be obtained with good resolution. Figure 6 displays photos of the formed PDMS square cavities, and as can be seen, no deformation occurred. The dimensions of the photopatterned PDMS cavities are in good accordance with the mask patterns. The thickness obtained for these microstructures was 69.22 μm ($\pm$0.83 μm in 5 measurements), a smaller value as compared to the ones measured for fully irradiated wafers without a profiler. This decrease was because of the pressure that was applied during the alignment. The thickness of 70 μm (see the middle and bottom photos in Figure 6) was well within the target range of 50$-$200 μm. Moreover, it was possible to design a similar square cavity with a thickness of 125 μm (see the top photo in Figure 6). Contrary to the method developed by Papautsky in which Sylgard 184 was used,[17] the present process necessitated no fine-tuning of the temperature and no baking time. Although the approach involved a radical pathway, it could, because of the choice to use very reactive acrylate and methacrylate moieties, be performed in air. It is noteworthy that oxygen diffusion becomes a problem only for thin layers, typically below 15 μm.[24]

Membrane. The adhesion of the walls to the silicon wafer appearing to be satisfactory, the next step consisted in obtaining the membrane. Two polysiloxanes grades were investigated: Sylgard 184, already largely used in microelectronics, and Zipcone TR, which is resistant at high temperature because of its formulation incorporating TiO_2 (Figure 7).

Both polymers can be cross-linked either at room or medium temperature (i.e., below 100 °C). To promote a good adhesion between different silicone layers, several possibilities exist: one can use either two already cross-linked surfaces that have been chemically modified, by mainly plasma treatment, or two partially cured surfaces. It is worth noting that the surface-anchoring chemistry of PDMS has been thoroughly studied to provide either specific reactivity or affinity patterns.[25−30] Moreover, both methods have been tested for the proposed device. In each case, the prepoly-

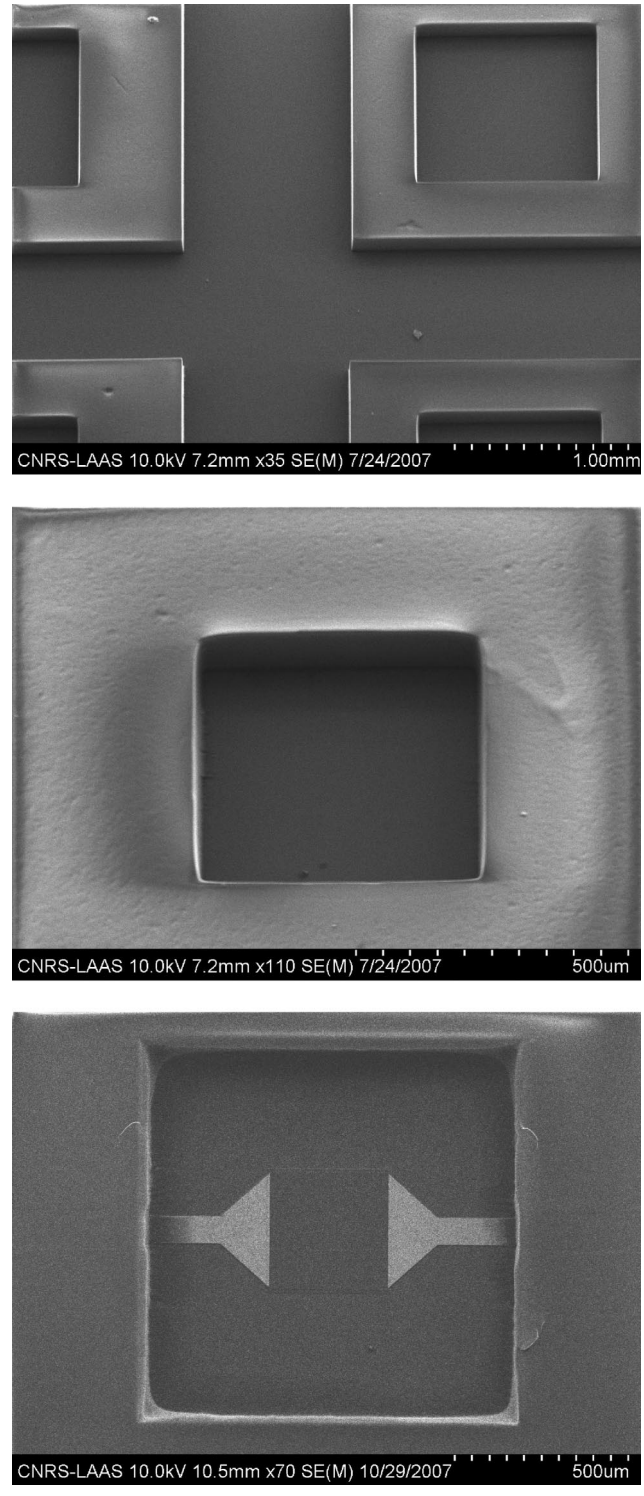

Figure 6. Pictures of the formed PDMS square cavities. Top, 1 mm × 1 mm × 125 μm cavities; middle a 500 μm × 500 μm × 70 μm cavity; bottom, a square cavity (500 μm × 500 μm × 70 μm, 4 in. wafer) with a resistance.

(20) Thibault, C.; Severac, C.; Mingotaud, A. F.; Vieu, C.; Mauzac, M. *Langmuir* **2007**, *23*, 10706–10714.
(21) Wong, A. K. Y.; Krull, U. J. *Anal. Bioanal. Chem.* **2005**, *383*, 187–200.
(22) Liu, L.; Engelhard, M. H.; Yan, M. *J. Am. Chem. Soc.* **2006**, *128*, 14067–14072.
(23) Barrio, R.; Maffiotte, C.; Gandia, J. J.; Carabe, J. *J. Non-Cryst. Solids* **2006**, *352*, 945–949.
(24) O'Brien, A. K.; Bowman, C. N. *Macromolecules* **2006**, *39*, 2501–2506.

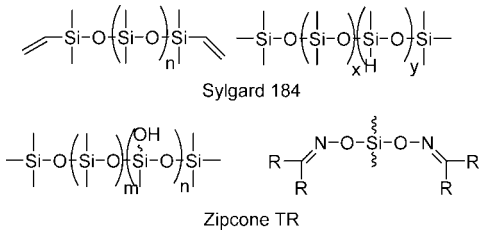

Figure 7. Reactive components of sylgard 184 and zipcone TR.

mer was spin-coated on a wafer with a polyethylene-terephtalate surface, and deposited on the walls by lamination using a process developed for SU-8 multi layers.[31] In the case of Sylgard 184, a standard O_2 plasma technique was applied in order to enhance the adhesion between the walls and the membrane. This plasma treatment was followed by an oven treatment at 65 °C for 1 h. An alternative consisted in partially curing the membrane and still performing a plasma treatment on the walls in the presence of the energetic material. Remarkably, the energetic material resisted the plasma treatment, which could be verified by depositing the energetic material on a resistance and exposing it to a short-sequence (30s) O_2 plasma. The resistance was then ignited and the energetic material decomposition was observed at the expected temperature. The main disadvantage of this technique was the poor reproducibility of the adhesion between the RMS 083 walls and the Sylgard 184 membrane. An alternative way would thus be to use Zipcone TR because it reacts through silanol and oxime functions. By a simple incorporation of silanol moieties in the RMS 083, the two layers could become covalently attached after a thermal treatment, because of the reaction of the silanols (in RMS 083 new formulation) and oxime groups (in Zipcone TR). Preliminary experiments have been tested under these conditions and proved to be successful. Although the plasma treatment may not be the best option, it was nonetheless possible to obtain a membrane that adhered correctly to the walls. Consequently, the fabrication of a first actuator prototype including the heating resistance, the energetic material, the walls, and the membrane could be achieved. This prototype is depicted in Figure 8.

Actuation. Once the heating platform and the device were obtained, the actuation was tested by applying a power of 100 mW to the resistance on a 1 mm × 1 mm system (Figure 9). Two droplets of the energetic material solution were deposited, which corresponded to 60 ng. The deformation of the membrane was observed by optical profilometry,[13] and

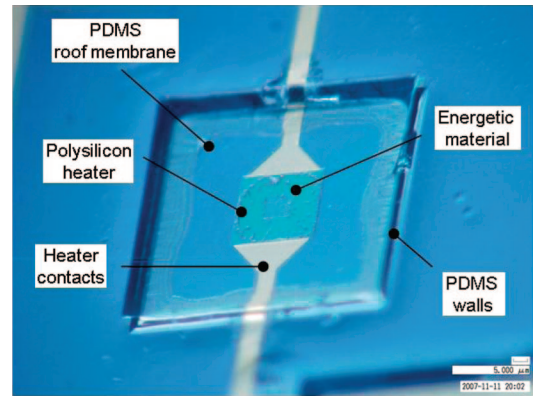

Figure 8. Picture of the final actuator with all its layers: the heating resistance, the energetic material, the walls, and the membrane.

it was noted that the membrane inflated before reaching a deformation height of 100 μm. It was determined by modeling that such a deformation should correspond to an injected water volume of 40 nL. The same procedure was repeated on an area of 500 μm × 500 μm with 90 ng of energetic material. A deformation of 46 μm was observed, which corresponded to an injected water volume of 5 nL. Compared to other actuators using propellant systems, this one is more compact with an area of 0.25 mm^2 compared to 6.25 mm^2 for ref 5 and 4 mm^2 for ref 6. Furthermore, the generated overpressure is higher for a lower applied energy: 13 kPa using 300 mWs (6V) compared to 3.5 kPa using 180mWs in ref 5 and 10 kPa using 9 V in ref 6. A more detailed discussion of the actuation characteristics can be found in ref 10.

During the actuation, it could be noted that the membrane inflated, reached a maximum level, after which a slight deflation was observed. This was explained by the cooling of the gases resulting from the decomposition of the energetic material. Both the explosion and diffusion of gases in the chamber are expected to occur within the range of a millisecond, a duration short enough to ensure a good actuation of the membrane. Indeed, it is possible to evaluate the time for half of the generated gases to pass through the membrane. This is done by the permeability coefficient, defined as

$$P = \frac{\text{permeant qty (cm}^3\text{ at 273 K and 1013 mbar)} \times \text{film thickness (cm)}}{\text{Area (cm}^2\text{)} \times \text{time (s)} \times \Delta P\text{ (Pa)}} \quad (1)$$

The permeability coefficient for PDMS at different temperatures can be found in the literature[32] (e.g., 476 × 10^{-13} cm^2 s^{-1} Pa^{-1} at 20 °C for dioxygen). Considering that 855 ng of energetic material leads to the formation of 1.15 × 10^{-8} moles of gases, the minimum time for half of this amount to pass through the membrane can be calculated in the range of several tens of seconds for a difference of pressure of 0.05 MPa at either 20 or 100 °C. It is noteworthy that no rupture of the membrane was observed during the actuation.

(25) Crowe, J. A.; Efimenko, K.; Genzer, J. *Science and Technology of Silicones and Silicone-Modified Materials*; ACS Symposium Series; American Chemical Society: Washington, D.C., 2007; Vol. 964, pp 222−255.
(26) Wu, D.; Qin, J.; Lin, B. *Lab Chip* **2007**, *7*, 1490–1496.
(27) Patrito, N.; McCague, C.; Norton, P. R.; Petersen, N. O. *Langmuir* **2007**, *23*, 715–719.
(28) Eddings, M. A.; Johnson, M. A.; Gale, B. K. *J. Micromech. Microeng.* **2008**, *18*, 067001.
(29) Bodas, D. S.; Kan-Malek, C. *Sens. Actuators, B* **2007**, *120*, 719–723.
(30) Wu, Y.; Huang, Y.; Ma, H. *J. Am. Chem. Soc.* **2007**, *129*, 7226–7227.
(31) Abgrall, P.; Lattes, C.; Conédéra, V.; Dollat, X.; Colin, S.; Gué, A. M. *J. Micromech. Microeng.* **2006**, *16*, 113–121.
(32) Pauly, S. In *Polymer Handbook* 3rd ed.; Brandrup, J., Immergut, E. H., Eds.; Wiley Interscience: New York, 1989; p VI/435.

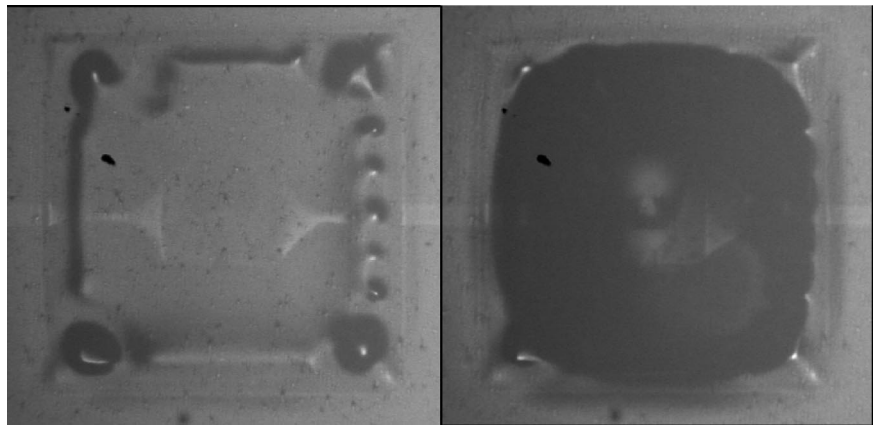

Figure 9. Actuator system with an area of 1 mm × 1 mm: left, before actuation; right, after actuation.

A video corresponding to the actuation can be found in the Supporting Information.

Conclusion

The fabrication of a microactuator was successfully carried out but more importantly, the technical key steps were resolved by chemistry. First, a facile synthesis of a "green" and stable energetic material was developed, and the synthesis could be performed in a clean room environment. Second, benefit was taken from the commercially available PDMS (RMS 083), by using it as a negative photoresist and covalently grafting it onto silicon wafers through an acryloxy functionalization of the surface. The next step involving a microfluidic integration has to be performed. The simple use of photolithographic masks enables a very rapid access to a prototype, which is essential in the development of new microelectronic processes. Finally, although literature often reports on surface functionalization of surfaces on small Si wafers, the present article demonstrates that it was possible to scale up the adhesion and photoirradiation process in order to use it for standard 4 in. wafers. The present actuator could be used, for instance, in spatial applications for the deployment of mechanical parts in small satellites or in biological or medical applications for microsyringes.

Acknowledgment. This work was supported by the CNRS and the French National Research Agency (programme blanc CSD1, ANR-05-BLAN-0301). The authors express their gratitude to Véronique Conédéra for her help in carrying out the photolithography. Many thanks are also due to CIBA for generously donating the photoinitiator.

Supporting Information Available: Two movies representing the decomposition of the energetic material on a chip and the actuation (MPG); technical details of the heating platform and of the photolithographic process (PDF). This material is available free of charge via the Internet at http://pubs.acs.org.

CM803146Y